A Computational Method for Internal Flows with Mixed Inlet-Outlet Ports, Application to Nozzle Flows in Melt-Spinning Processes

B. Koren [1] and D. Lanser [2]

Abstract. A numerical method for computing the compressible air flow in a nozzle is briefly presented. The nozzle is used for drawing fibers in so-called melt-spinning processes. The flow model consists of the 2-D, steady, compressible Navier-Stokes equations in Cartesian coordinates. The discretization and solution method are standard. Yet, some new numerical ingredients have to be applied: a boundary-condition treatment for mixed inlet-outlet ports (a treatment which admits the unconstrained occurrence of a vortex at a boundary) and a technique for improving the condition of the system of discrete equations in low-Mach number regions. The numerical method is applied to a simplified part of the nozzle. It is promising as far as more realistic computations are concerned.

1 INTRODUCTION

Melt spinning is a process to make non-woven cloth, a basic product in the production of many other products, ranging from carpets and roofings to wound-dressings. At the start of the process, a polymer is melted and extruded into a large set of very thin fibers, which are drawn by a high-subsonic air flow, through the nozzle considered (Figure 1). The air flow in the nozzle is fed from two tanks of pressurized air, both with a downward-directed outlet channel with its mouth in the upper part of the nozzle wall (Figure 1). Below the nozzle, the fibers are laid down, in a random pattern, on a moving belt. The final industrial goal of the present work is to have an aerodynamic design tool for the nozzle, in order to reduce its relatively large running costs (without diminishing the tractive force exerted on the fibers). For this purpose, the availability of a robust computational method for internal aerodynamics, with mixed inlet-outlet ports, is a prerequisite. In the present paper, such a method is briefly presented.

A difficulty of computing the air flow in the nozzle is that little a-priori knowledge exists about the velocity field, for given pressures in the two pressure chambers. For small pressure variations (in the pressure chambers), strong qualitative changes may be expected in flow topology and magnitudes of flow speeds. Because we want to make use of a single computational method and because of the expected large qualitative solution changes, this method must be robust. No off-the-shelf CFD-code was known, which could meet the foreseen robustness requirements. Therefore, on the basis of an existing method, the present robust, special-purpose method was developed.

The contents of the paper is the following. In Section 2, the computational domain, the flow equations and corresponding boundary conditions are given. In Section 3, the discrete flow model is summarized. In Section 4, the solution method for the discrete equations is given and in Section 5, flow solutions are presented.

2 FLOW MODEL

2.1 Geometry

The sizes of the nozzle as sketched in Figure 1 are not correct. In reality, the nozzle is much more slender; the length-width ratio is about 300:1. The geometry of the nozzle is exactly symmetric. Hence, we can consider the half problem only (see Figure 1 for the coordinates to be used). For simplicity, we refrain from computing the

[1] CWI, P.O. Box 94079, 1090 GB Amsterdam, The Netherlands
[2] CWI, P.O. Box 94079, 1090 GB Amsterdam, The Netherlands

© 1998 B. Koren and D. Lanser
ECCOMAS 98.
Published in 1998 by John Wiley & Sons, Ltd.

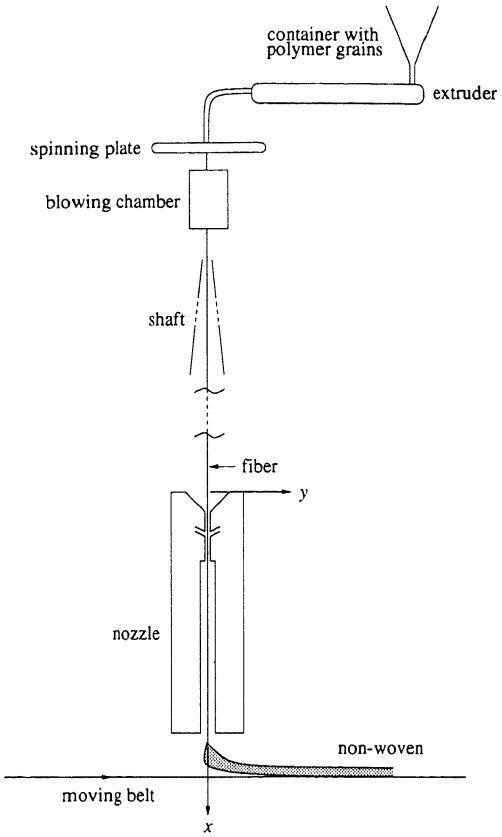

Figure 1. Schematic representation of the production process of non-wovens.

flow in the outlet channel of the pressure chamber. An approximate solution of this outlet flow is directly imposed as inlet boundary condition at the corresponding part of the nozzle wall. To start with, the entire nozzle wall is taken flat, i.e., the backward-facing step in the nozzle wall (Figure 1) is not (yet) considered. The fiber inlet and outlet ports of the nozzle are taken as upper and lower boundaries of the computational domain, respectively. Not taking real far-field upper and lower boundaries, but these relatively near-field boundaries instead, is computationally efficient.

2.2 Flow equations

To start, the 2D, viscous, compressible nozzle flow is assumed to be steady and laminar. As the governing equations we take the full, perfect-gas Navier-Stokes equations

$$\frac{\partial f(q)}{\partial x} + \frac{\partial g(q)}{\partial y} - \frac{1}{\mathrm{Re}}\left(\frac{\partial r(q)}{\partial x} + \frac{\partial s(q)}{\partial y}\right) = 0, \quad (1)$$

with the conservative state vector $q = (\rho,\rho u,\rho v,\rho e)^T$ and the total energy $e = \frac{1}{\gamma-1}\frac{p}{\rho} + \frac{1}{2}(u^2+v^2)$, $\gamma = \frac{7}{5}$. The convective flux functions $f(q)$ and $g(q)$ are

$$f(q) = \begin{pmatrix} \rho u \\ \rho u^2 + p \\ \rho uv \\ \rho u(e + \frac{p}{\rho}) \end{pmatrix}, \quad (2)$$

$$g(q) = \begin{pmatrix} \rho v \\ \rho vu \\ \rho v^2 + p \\ \rho v(e + \frac{p}{\rho}) \end{pmatrix} \quad (3)$$

and the diffusive flux functions,

$$r(q) = \begin{pmatrix} 0 \\ \tau_{xx} \\ \tau_{xy} \\ u\tau_{xx} + v\tau_{xy} + \frac{1}{\gamma-1}\frac{1}{\mathrm{Pr}}\frac{\partial c^2}{\partial x} \end{pmatrix}, \quad (4)$$

$$s(q) = \begin{pmatrix} 0 \\ \tau_{xy} \\ \tau_{yy} \\ v\tau_{yy} + u\tau_{xy} + \frac{1}{\gamma-1}\frac{1}{\mathrm{Pr}}\frac{\partial c^2}{\partial y} \end{pmatrix}, \quad (5)$$

with the speed of sound $c = \sqrt{\frac{\gamma p}{\rho}}$ and the viscous stresses $\tau_{xx} = \frac{4}{3}\frac{\partial u}{\partial x} - \frac{2}{3}\frac{\partial v}{\partial y}$, $\tau_{xy} = \frac{\partial u}{\partial y} + \frac{\partial v}{\partial x}$ and $\tau_{yy} = \frac{4}{3}\frac{\partial v}{\partial y} - \frac{2}{3}\frac{\partial u}{\partial x}$.

In the definition of the Reynolds number Re, we take as the characteristic density and viscosity those of the ambient air out of the nozzle. For the characteristic speed, the speed of sound of the ambient air is taken and for the characteristic length, the half width of the nozzle.

2.3 Boundary conditions

2.3.1 At vertical boundaries

The conditions to be imposed at the two vertical nozzle boundaries are rather trivial. At the symmetry boundary, the symmetry condition is imposed. So far, the fibers, which are all located on this boundary, are supposed to have no influence on the nozzle flow. At the boundary opposite to the symmetry plane, the impermeable, solid-wall condition is imposed, except for the pressure-chamber outlet, of course. There, inflow conditions are prescribed: a Poiseuille-type inflow with the maximum Mach number equal to 1. The situation at the pressure chamber outlet is sketched in Figure 2. The geometrical width of the small tube from the pressure chamber outlet

to the nozzle is constant, but the aerodynamic width is not. Given the boundary-layer growth in the tube, it is smallest at the last cross section (section 1 in Figure 2). We assume the tangential velocity component at this position to be parabolic and the normal velocity component to be zero. Since the pressure chamber temperature is accurately known, it seems appropriate to make an estimate for the temperature at section 1 through 1D gas dynamics theory (through the relation $\frac{T_t}{T} = 1 + \frac{\gamma-1}{2}M^2$, with M equal to 1 and T_t equal to the known pressure chamber temperature). The three conditions, which are thus known at section 1, are simply extrapolated to section 2 (Figure 2) and imposed there as subsonic inflow boundary conditions. (The possibility of expansion to supersonic speeds, into the direction of section 2, of the mixed subsonic-sonic flow at section 1, is not considered.)

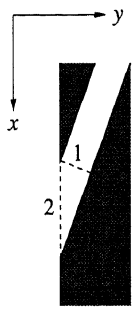

Figure 2. Pressure chamber outlet.

2.3.2 *At horizontal boundaries*

The boundary-condition treatment at the remaining upper and lower boundaries is less trivial and very important for nozzle designers. For a given outflow from the pressure chamber, it is not a-priori known for – in particular – the upper nozzle boundary, whether it will be an air-inlet boundary, a mixed inlet-outlet boundary, or even an air-outlet boundary. The nozzle configuration may be interpreted as an upside-down chimney of a furnace, with as the furnace outlet the pressure tank outlet. As it is not a-priori known for a chimney, how effective it will be in ejecting soot, for the present nozzle it is a-priori unknown how effective it will be in ejecting the fibers. A physically and numerically proper treatment of both the upper and lower boundary is important for getting to know this. Unconstrained capturing of pure inflow, mixed inflow-outflow, or pure outflow requires that the velocity component normal to the boundary is *not* imposed. I.e., at both the upper and lower boundary, u must be left free. To ensure next a good capturing of subsonic inflow, which requires the most, i.e., three boundary conditions, the complete thermodynamic state must be prescribed, still leaving free: one kinematic boundary condition. This kinematic condition can be, e.g., the tangential velocity component v, the inflow direction $\frac{v}{u}$, or the magnitude of the inflow velocity $\sqrt{u^2+v^2}$. We choose the first possibility; at both the upper and lower boundary we take $v = 0$. The thermodynamic quantities at both boundaries are taken equal to the known static, ambient air conditions. In reality, the thermodynamic conditions at the boundaries will be perturbed. E.g., at inflow, the real pressure and density will be lower than the static conditions. We assume that these perturbations are small enough to be neglected at first.

3 DISCRETE EQUATIONS

For a detailed description of the discretization method, we refer to [2]. In this section, a summary is given.

The Navier-Stokes equations (1)-(5) are discretized in their integral form. A straightforward and simple discretization of the integral form is obtained by subdividing the computational domain into (quadrilateral, cell-centered) finite volumes and by requiring that the integral form holds for each finite volume separately. This discretization requires an evaluation of the convective and diffusive flux vector at each finite-volume wall.

3.1 Evaluation of convective fluxes

For the evaluation of the convective fluxes, for the present flow problem, a scheme is to be preferred, which (i) respects physics because of the delicate upper and lower boundaries and the high Reynolds number (based on the tiny nozzle width Re is $\mathcal{O}(10^4)$), and which (ii) has good robustness properties. Given these requirements, we choose an upwind approach. In here, the convective flux is assumed to be constant along each cell face, and to be determined by a uniformly constant left and right state only. For the 1D Riemann problem thus obtained, an approximate Riemann solver is applied, viz. Osher's [4]. These days, it is well-known that for an accurate resolution of shear flows, flux-difference splitting schemes are to be preferred above flux-vector splitting schemes. In [6], evidence has been given for this.

3.2 Evaluation of diffusive fluxes

For the evaluation of the diffusive fluxes, the standard central technique, as outlined in [5], is applied. For the

necessary computation, at each finite-volume wall, of Δu, Δv and Δc^2, the technique uses a shifted volume wall overlying the finite-volume wall considered.

4 SOLUTION METHOD

4.1 Brief outline

The solution method for the system of discretized Navier-Stokes equations is multigrid-accelerated point Gauss-Seidel relaxation [1]. This method has proved to work fine for various standard test cases from gas dynamics. However, an inhibitor for good convergence of this solution method is formed by flow regions with low Mach numbers. For the present application, these are the low-speed regions along the solid walls and in the viscous kernels of vortices. Convergence rates which deteriorate with decreasing Mach numbers are not specific to multigrid methods, but appear to occur for any solution method. The cause has to be sought in the convective part of the continuous Navier-Stokes equations, in their increasing stiffness.

In our case, in the zero-Mach-number limit, point-relaxation methods for solving the discretized steady Navier-Stokes equations will suffer from the ill-conditioning of the corresponding derivative matrix to be inverted. In [3], for the Euler equations, it has been shown that the nearly singular matrix to be inverted, can be regularized by adding another singular matrix to it, yielding a matrix which is very regular and, still, does not slow down too much the quadratic convergence of the exact Newton iteration. In the present Navier-Stokes work, the same fix is applied to regularize the Navier-Stokes derivative matrix in low-Mach number regions. In the next section, we give a short description of this fix for the clarifying limit case of the 2D Euler equations.

4.2 Condition improvement for low Mach numbers

To get some evidence of the poor conditions mentioned in the previous section, consider $\frac{1}{\mathrm{Re}} = 0$, $0 < u < c$, $0 < v < c$, square finite volumes with i and j the running indices in positive x- and y-direction, respectively, and a first-order upwind discretization. Then, one can derive as iteration formula for, e.g., a downstream relaxation sweep:

$$(|A| + |B|)(\tilde{q}^{n+1}_{i,j} - \tilde{q}^{n}_{i,j}) = -A^{+}(\tilde{q}^{n}_{i,j} - \tilde{q}^{n+1}_{i-1,j}) - A^{-}(\tilde{q}^{n}_{i+1,j} - \tilde{q}^{n}_{i,j}) + -B^{+}(\tilde{q}^{n}_{i,j} - \tilde{q}^{n+1}_{i,j-1}) - B^{-}(\tilde{q}^{n}_{i,j+1} - \tilde{q}^{n}_{i,j}), \quad (6)$$

where $\tilde{q}$ is the entropy-variable state vector, defined by $\mathrm{d}\tilde{q} = \left(\frac{1}{\rho c}\mathrm{d}p, \mathrm{d}u, \mathrm{d}v, \mathrm{d}p - c^2\mathrm{d}\rho\right)^T$, n the relaxation sweep counter and $|A| + |B|$ the matrix to be inverted:

$$|A| + |B| = A^{+} - A^{-} + B^{+} - B^{-} = \quad (7)$$

$$\begin{pmatrix} 2c & u & v & 0 \\ u & v+c & 0 & 0 \\ v & 0 & u+c & 0 \\ 0 & 0 & 0 & u+v \end{pmatrix}. \quad (8)$$

For the definition of A^{+}, A^{-}, B^{+} and B^{-}, we refer to [3], where it is also shown that for the upstream relaxation sweep, $|A| + |B|$ also occurs as the matrix to be inverted. For the condition K of $|A| + |B|$, it follows from (7)

$$K = \max\left(\frac{3+\sqrt{1+4M^2}}{2M}, \frac{3+\sqrt{1+4M^2}}{3-\sqrt{1+4M^2}}\right), \quad (9)$$

with M the Mach number. So, $|A| + |B|$ is singular at $M = 0$. To regularize $|A| + |B|$, as mentioned, one can simply add another singular matrix R to it, leading to the approximate derivative matrix

$$(|A| + |B|)_R = |A| + |B| + R. \quad (10)$$

By taking

$$R = \begin{pmatrix} 0 & 0 & 0 & 0 \\ 0 & 0 & 0 & 0 \\ 0 & 0 & 0 & 0 \\ 0 & 0 & 0 & c-u-v \end{pmatrix}, \quad (11)$$

the singularity at $M = 0$ is removed. For the condition K_R of $(|A| + |B|)_R$, it is found

$$K_R = \max\left(\frac{3+\sqrt{1+4M^2}}{2}, \frac{3+\sqrt{1+4M^2}}{3-\sqrt{1+4M^2}}\right). \quad (12)$$

Note that thanks to the close resemblance of $|A|+|B|$ and $(|A| + |B|)_R$, the possible convergence deterioration is expected to be marginal. For details about the conservative implementation of this additive conditioning, we refer to [3].

5 NUMERICAL RESULTS

An impression is given of the performance of the numerical method. In Figures 3 and 4, for a sequence of three increasing Reynolds numbers (Re = 10^3,10^4,10^5), we give velocity-vector and Mach-number distributions in the neighborhood of the pressure chamber outlet. (The outlet is located at $y = 1$, $15.63 \leq x \leq 16.37$.) For both lower Reynolds-number cases, the upper boundary of the

nozzle appears to be a mixed inlet-outlet port, with the outflow located at the side of the symmetry plane ($y = 0$), i.e., along the fibers. This leads to a negative contribution to the net pull performed on the fibers. In Figures 5 and 6, computational results are shown for a fixed value of Re (Re=2.4 $\times$ 10^4), but for other geometries: nozzles with subsonic outlet diffusor. The nozzles with diffusor appear to perform better with respect to fiber drawing.

The convergence results and the computing times needed are satisfactory. Given this result, as well as the apparent reliability of the numerical solutions, the computational method seems to be an appropriate tool for design purposes.

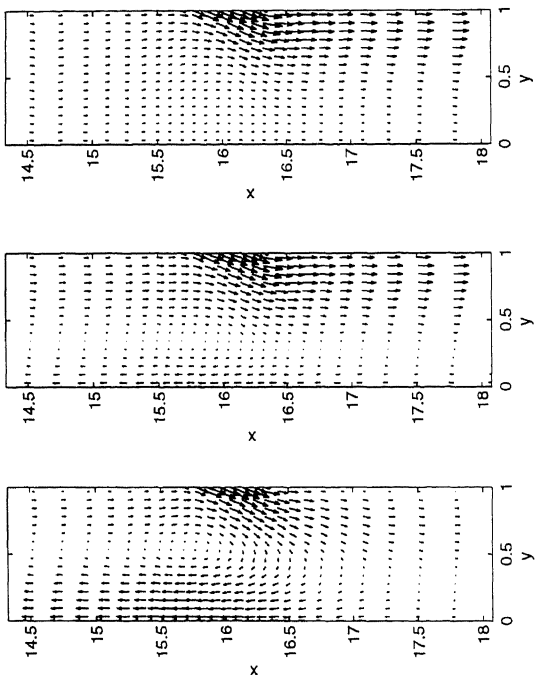

Figure 3. Velocity-vector distributions around pressure-chamber outlet port for, from below to above, Re=10^3,10^4,10^5.

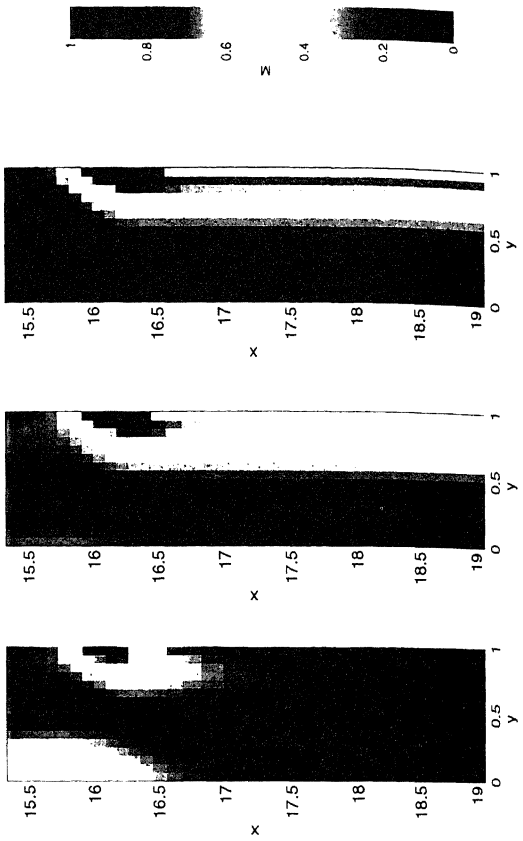

Figure 4. Mach-number distributions around pressure-chamber outlet port for, from below to above, Re=10^3,10^4,10^5.

REFERENCES

[1] B. Koren, 'Multigrid and defect correction for the steady Navier-Stokes equations', *Journal of Computational Physics*, **87**, 25–46, (1990).

[2] B. Koren, 'Upwind discretization of the steady Navier-Stokes equations', *International Journal for Numerical Methods in Fluids*, **11**, 99–117, (1990).

[3] B. Koren, 'Condition improvement for point relaxation in multigrid, subsonic Euler flow computations', *Applied Numerical Mathematics*, **16**, 457–469, (1995).

[4] S. Osher and F. Solomon, 'Upwind difference schemes for hyperbolic systems of conservation laws', *Mathematics of Computation*, **38**, 339–374, (1982).

[5] R. Peyret and T.D. Taylor, *Computational Methods for Fluid Flow*, Springer, Berlin, 1983.

[6] B. van Leer, J.L. Thomas, P.L. Roe, and R.W. Newsome. A comparison of numerical flux formulas for the Euler and Navier-Stokes equations. AIAA paper 87-1104.

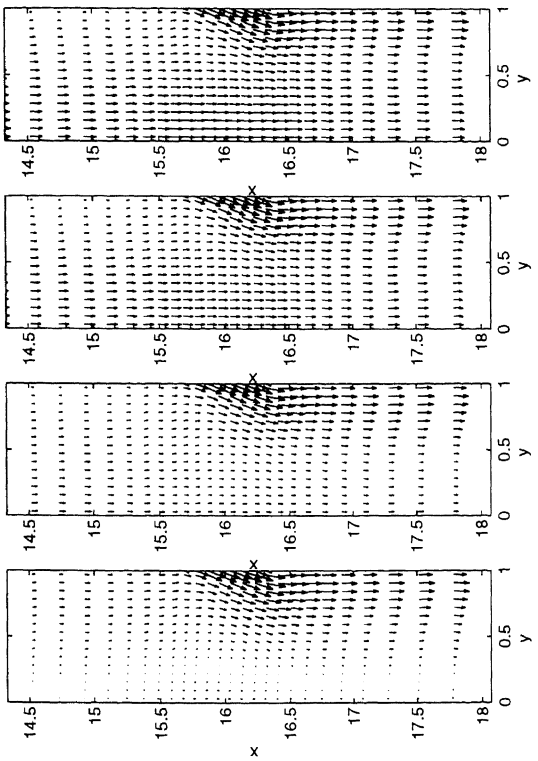

Figure 5. Velocity-vector distributions around pressure-chamber outlet port for Re=2.4 × 10^4 and four different geometries.

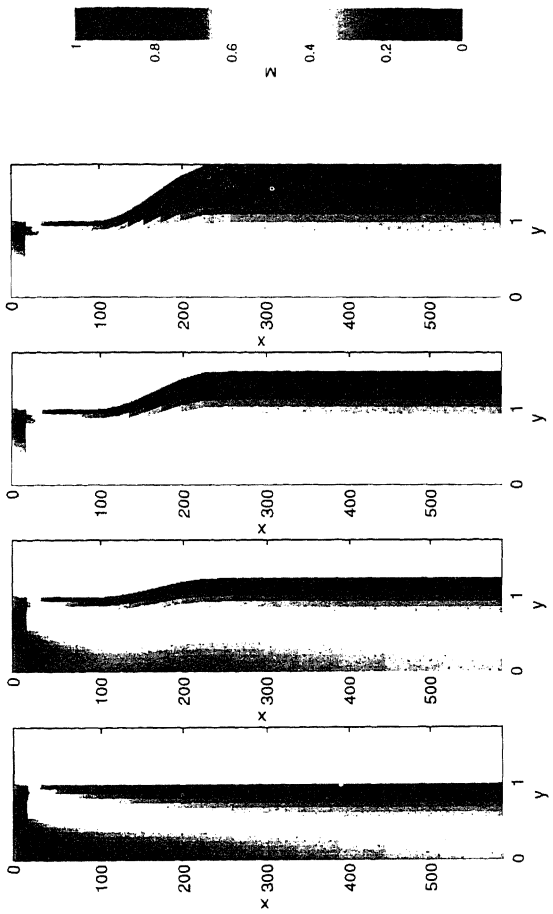

Figure 6. Mach-number distributions in entire nozzle, for Re=2.4 × 10^4 and four different geometries.